Remote Sensing in Ecology and Conservation
Open Access
ZSL LET'S WORK FOR WILDLIFE

ORIGINAL RESEARCH

A simple method for estimating the effective detection distance of camera traps

Tim R. Hofmeester[1], J. Marcus Rowcliffe[2] & Patrick A. Jansen[1,3]

[1]Department of Environmental Sciences, Wageningen University, Wageningen, the Netherlands
[2]Institute of Zoology, Zoological Society of London, London, United Kingdom
[3]Center for Tropical Forest Science, Smithsonian Tropical Research Institute, Balboa, Ancon, Republic of Panamá

Keywords
Body mass, camera traps, distance sampling, passive infrared sensor, sensor sensitivity, trail camera

Correspondence
Tim R. Hofmeester, Department of Environmental Sciences, Wageningen University, P.O. Box 47, 6700 AA, Wageningen, the Netherlands.
Tel: +31 317485828; Fax: +31 317484545;
E-mail: tim.hofmeester@wur.nl

Funding Information
This work was funded by the Netherlands Ministry of Health, Welfare and Sport.

Editor: Rob Williams
Associate Editor: Natalie Kelly

Received: 15 March 2016; Revised: 13 July 2016; Accepted: 28 July 2016

doi: 10.1002/rse2.25

Abstract

Estimates of animal abundance are essential for understanding animal ecology. Camera traps can be used to estimate the abundance of terrestrial mammals, including elusive species, provided that the sensitivity of the sensor, estimated as the effective detection distance (EDD), is quantified. Here, we show how the EDD can be inferred directly from camera trap images by placing markers at known distances along the midline of the camera field of view, and then fitting distance-sampling functions to the frequency of animal passage between markers. EDD estimates derived from simulated passages using binned detection distances approximated those obtained from continuous detection distance measurements if at least five intervals were used over the maximum detection distance. A field test of the method in two forest types with contrasting vegetation density, with five markers at 2.5 m intervals, produced credible EDD estimates for 13 forest-dwelling mammals. EDD estimates were positively correlated with species body mass, and were shorter for the denser vegetation, as expected. Our findings suggest that this simple method can produce reliable estimates of EDD. These estimates can be used to correct photographic capture rates for difference in sampling effort resulting from differences in sensor sensitivity between species and habitats. Simplifying the estimation of EDD will result in less biased indices of relative abundance, and will also facilitate the use of camera trap data for estimating animal density.

Introduction

Estimation of animal abundance is essential for understanding animal ecology and for wildlife management and conservation. However, for many species (e.g., forest-dwelling mammals, elusive carnivores) conventional techniques such as capture–mark–recapture or line transect counts are difficult and time consuming (Wilson and Delahay 2001). Cameras with passive infrared (PIR) sensors, commonly referred to as camera traps or trail cameras, can detect rare, cryptic and elusive animals and are increasingly used to detect and monitor wildlife worldwide (Rowcliffe and Carbone 2008). PIR sensors detect a difference in heat and motion between subjects and the environment and trigger the camera if the difference exceeds a pre-set threshold (Rovero et al. 2013). Thus, animals that are warmer than their surroundings will trigger the camera when passing within the range of the sensor and are photographed or filmed.

When animals can be individually identified, camera traps can be used to perform conventional capture–mark–recapture using the capture rate of known individuals (Karanth and Nichols 1998). For animals that cannot be distinguished individually, camera traps are often used to derive relative abundance estimates, reasoning that photographic capture rates – the number of visits recorded per unit time – of a species will be proportional to its abundance (Carbone et al. 2001). However, the use of capture

rates as relative abundance indices has received criticism, as capture rates are influenced by other factors besides animal abundance, which can lead to important biases (e.g., Sollmann et al. 2013). Some of these factors are related to non-random movement of the focal species, such as the preferred use of trails. However, most factors that bias capture rates are related to the PIR sensor of the camera trap: camera type, camera placement, animal size, vegetation density, temperature and relative humidity all influence the effective range of the sensor (Kelly and Holub 2008; Rowcliffe et al. 2011). Some of these factors can be dealt with using adequate sampling design, for example, using the same camera model and thus the exact same PIR sensors (Rovero et al. 2013), the same sampling period, similar climate and random sampling points (Kelly and Holub 2008; Sollmann et al. 2013). However, when the goal is to compare different species, or the same species in different habitat types, biases may remain a problem.

Although larger animals omit less heat per unit of mass than small animals, they still omit a larger absolute amount of heat (thermal infrared) than do small animals (Mcnab 1980). Therefore, the PIR sensor of a camera trap is more sensitive to large animals than to smaller animals (Rowcliffe et al. 2011). Furthermore, most PIR sensors are more sensitive in the middle of the field of view (FOV) than at the edges (Rovero et al. 2013), which also results in differences in detectability between large and small species (Rowcliffe et al. 2011). The resulting differences in sampling area can be corrected for by estimating the effective detection distance (EDD) and angle for each species (Rowcliffe et al. 2011). The EDD is the distance at which the number of animals detected further away equals the number of animals missed nearer by. The estimation of EDD and angle is essential for using the Random Encounter Model (REM; Rowcliffe et al. 2008), which estimates animal densities by correcting photographic capture rates for detection bias and species' day range. Rowcliffe et al. (2011) measured distances and angles by tracking the movement path of animals through the FOV on site, and measuring the distance and angle from the camera at first detection, which required a substantial investment of field time. This method was recently simplified by the use of a photograph of a grid of markers taken after each camera deployment to estimate detection distance and angle using image processing software (Caravaggi et al. 2016).

Here, we present an further simplified method to estimate the EDD directly from camera trap images. The principle is to establish markers at known distances along the midline of the FOV, record the frequency of animal passage between markers and then fit distance-sampling functions to distance distributions to estimate EDD. To determine whether this approach was effective, we compared it with the conventional method described by Rowcliffe et al. (2011) using simulated data. Then, in a field study, we tested whether EDD estimates derived with the line marker method (1) increased with body mass, as larger animals emit more infrared radiation; and (2) were shorter in denser vegetation, as vegetation affects transmission of infrared radiation.

Materials and Methods

We approached detection of animals by camera traps using distance-sampling detection models (sensu Rowcliffe et al. 2011). The trigger threshold of the PIR sensor of a camera trap is more easily exceeded by a warm-blooded animal walking close to the sensor than by an animal walking further away from the sensor. When we assume that an animal walking against the camera (distance of zero) is always detected, we can model the probability of being detected as a standard monotonically declining detection model. When the distance from the camera to each animal triggering the camera is known, these distances can be used as input for the detection model. Although exact distances are hard to obtain, distance classes are easily obtained from the images if intervals are marked in the FOV, and using distance classes is general practice in distance sampling (Buckland et al. 2015). Distance classes can be realized by establishing markers at known distances along lines running away from the camera when the camera is setup. As it is not practical to place such lines along multiple angles in the full FOV, we reasoned that the distance at which an animal triggers the camera and the distance at which an animal walks through the middle of the FOV are correlated. If this assumption holds, detection distance can be estimated by placing a line of markers in the middle of the FOV. We tested this assumption using a simulation (see below).

Distance data are obtained during annotation of the photographs, as the analyst records between which markers photographed animals pass, assigning each passage to a distance interval. All triggers of animals that do not cross the midline are ignored. The distribution of passages over the different distance categories is then used to fit a detection probability function from which EDD can be estimated using standard techniques for estimating effective strip width (line model) or effective detection radius (point model; Buckland et al. 2001). Where a line model assumes that the histogram of the number of detections over the different distance categories follows a distribution similar to the detection probability, a point model assumes that the distribution of the histogram is similar to the detection probability multiplied by the distance, correcting for the increase in detection area with distance. In our case, the detection along a centre line

may be best described by a line model, whereas the true detection by the sensor may be better described by a point model (Rowcliffe et al. 2011). Because the reduction of a cone-shaped detection area to a line might not result in a perfect line detection, we considered both models in our analysis. The fitting of detection probability functions to distance data can be done with several software packages such as DISTANCE (Thomas et al. 2010) or the R package *mrds* (Laake et al. 2015).

Following Rowcliffe et al. (2011) we use two different detection probability models: A half-normal model and a hazard-rate model, respectively:

$$g(x) = \frac{\exp(-x^2)}{2\alpha^2} \quad (1)$$

$$g(x) = 1 - \exp\left(-\left(\frac{x}{\alpha}\right)^{-\gamma}\right) \quad (2)$$

where $g(x)$ is the detection probability at distance x, α defines the width of the function and γ the shape of the hazard-rate function. These detection functions can also be expanded using covariates, such as body mass, habitat type or season (Rowcliffe et al. 2011). We fitted both simple distance-sampling models without covariates on single species in each habitat, and multiple-covariate distance-sampling models, including body mass and habitat as covariates (see below; Marques and Buckland 2003). We selected the best-performing models based on Akaike's Information Criterion (AIC) values as estimates of model quality (Buckland et al. 2015).

Simulation

To determine whether EDD estimated using grouped distances along the centre line reflects EDD as estimated by the baseline approach described by Rowcliffe et al. (2011) using direct radial distances, we bootstrapped simulated samples, and explored the effect of varying the number of intervals used. For each of 1000 samples, we defined 100 random positions of first detection (point of trigger) by drawing radii from a hazard-rate distribution and angles from a half-normal distribution. We then assigned each position a random direction of travel (uniform in 0–2π), and calculated the distance at which its trajectory crossed the camera's line of sight (centre-line distance). To define trajectories that could be observed to cross the camera's line of sight, we retained those that crossed the centre line in front of the camera, within the maximum trigger position distance, and after the point of trigger.

For each sample, we fitted a point detection function model to the direct trigger distance data to provide baseline expected EDD, using previously published methods (Rowcliffe et al. 2011). For comparable centre line models, we fitted both point and line models with data either binned into 2, 3, 4, 5 or 10 equal distance intervals, or unbinned using a grouped likelihood for the binned models (Buckland et al. 2001). In all cases we used hazard-rate models with no expansion terms. We tested with different numbers of distance intervals, as to assess what number of markers should be used in the field to obtain reliable EDD estimates. Here, we did not use expansion terms, as to enable a more robust estimation of EDD with low sample size.

Field test

We field tested the method by surveying mammals in forests that had contrasting densities of understory vegetation: four 1-ha plots with Scots pine (*Pinus sylvestris*) and a thick undergrowth of blueberry (*Vaccinium myrtillus*; dense understory), and four with Pedunculate oak (*Quercus robur*) with a sparse undergrowth of ferns (*Dryopteris dilatata*; open understory), scattered across the Netherlands (Table S1). Within each plot, we deployed two camera traps (HC500, RECONYX Inc., Holmen, WI) for 4 weeks, at two random locations >30 m apart. These cameras were moved to two new locations every 4 weeks until 14–18 different locations were sampled. Cameras were deployed on the tree nearest to a computer-generated random point, 40 cm above the ground facing north and aimed parallel to the ground. If necessary, we pruned the vegetation that blocked the view of the camera in a strip of 1 m broad and 5 m long in front of the camera. Vegetation was cut at 20–30 cm height to reduce false triggers due to moving vegetation which is standard practice in camera-trapping studies (Meek et al. 2014). Cameras were set to take a series of 10 photographs when triggered, and to be available for re-triggering without delay, so that movement between the markers would be recorded. Markers (bamboo sticks of 60 cm length) were placed in front of the camera, at intervals of 2.5 m, based on the maximum distance at which the cameras could detect a human (15 m). The markers were topped with two strips of black tape to increase visibility of the sticks in the photographs (Fig. 1). We placed the sticks slightly out of line, to ensure that they were all visible in the pictures. Depending on visibility through the vegetation, we used three to five markers, resulting in four to six distance intervals.

Photographs were managed and annotated using a custom-made photo-processing tool called 'Agouti' (cf. Kays et al. 2009). All photographs were automatically grouped into sequences if ≤5 min passed between triggers, stored as separate sequences if separated more than 15 min and otherwise checked manually to determine if it was the same or a different passage that triggered the camera. For each sequence, we noted the species and separated or combined sequences if the automatic procedure grouped or split passages from the same individual or group of

Figure 1. Camera trap photograph with a transect of markers at 2.5 m, 5 m, 7.5 m and 10 m, and a passing red fox (*Vulpes vulpes*).

individuals. Furthermore, we noted, for each individual animal, if it crossed the midline of the FOV, and if so, through which interval they passed. If the animals passed just behind the last marker, we noted it as passing in an interval of 2.5 m behind the last marker. There were no animals that triggered the camera and passed the line >2.5 m past the last marker.

All analyses were done in R 3.2.3 (R Core Team, 2015). We used a two-step approach, where we first estimated EDD for each species – habitat combination of which we had at least 20 distance measurements (Table 1), using models without covariates as implemented in the *mrds* package version 2.1.14 (Laake et al. 2015). We estimated EDD using point models, as these gave the best fit in our simulation (see results). EDD was estimated as:

$$\mathrm{EDD} = \mathrm{w} * \sqrt{\mathrm{Pa}}$$

where *w* is the truncation distance, and *Pa* is the expected probability of detection for an animal within distance *w* from the camera (Buckland et al. 2015), which is given as output of the *ddf* function in the *mrds* package. We used the furthest distance at which an animal was detected as the truncation distance.

A single body mass estimate per species was taken from the PanTHERIA database (Jones et al. 2009). As the exact

Table 1. Body mass, number of distance measurements obtained and total number of passes per habitat type for 13 forest mammal species that were detected during this study.

		Number of distance measurements/Total number of animals detected	
Species	Body mass (kg)[1]	Dense understory	Open understory
Eurasian red squirrel *Sciurus vulgaris* (squirrel)	0.3		7/9
European hedgehog *Erinaceus europaeus* (hedgehog)	0.8		2/8
Polecat *Mustela putorius* (polecat)	1.0		4/5
European pine marten *Martes martes* (pine marten)	1.3	**26**/33	**32**/41
Stone marten *Martes foina* (stone marten)	1.7		9/9
Feral cat *Felis catus* (cat)	2.9		**21**/24
European hare *Lepus europaeus* (hare)	3.8	2/4	**148**/199
Red fox *Vulpes vulpes* (fox)	4.8	**34**/39	**103**/132
European badger *Meles meles* (badger)	11.9	14/18	**54**/68
Roe deer *Capreolus capreolus* (roe deer)	22.5	**83**/108	**552**/763
Fallow deer *Dama dama* (fallow deer)	57.2	**108**/131	3/3
Wild boar *Sus scrofa* (wild boar)	84.5	**551**/633	
Red deer *Cervus elaphus* (red deer)	240.9	**390**/460	

Detection distance sample sizes above 20 are printed in bold. Abbreviated common names in brackets are used hereafter.
[1]Body mass values as given in the PanTHERIA database (Jones et al. 2009).

relationship between being detected by the camera and body mass was not known, we tested different transformations of body mass (square root, cube root and $\log_{10}$). The relationship between species-specific EDD estimates and transformed body mass was modelled with least-squares regression for each habitat. We used transformed parameters in a least-squares regression to be able to use the outcome as a linear covariate in the distance-sampling model. Secondly, we estimated EDD using multiple-covariate distance sampling (Buckland et al. 2015) with transformed body mass and habitat as covariates. Both covariates were modelled as additive to the scale parameter of the detection function. For this analysis we used all distance estimates, from all species in both habitats. The advantage of using a model including covariates is that all distance measurements for all species can be used. This enables the estimation of EDD for species for which we had too few measurements for fitting single-species models (Table 1).

Results

Simulation

We found that point models applied to centre-line data (Fig. 2) matched predetermined EDD fairly well (off 5% on average), whereas line models (Fig. S1) produced overestimates (by about 34% on average). Expected EDD was somewhat sensitive to the number of intervals used in centre-line models at very small interval numbers, with higher estimates on average using only two intervals, but no change in the expectation above three intervals. With three or four intervals there was a tendency for models to fit poorly, giving extremely low EDD estimates on occasion. With five or more intervals, the result was effectively indistinguishable from the unbinned analysis.

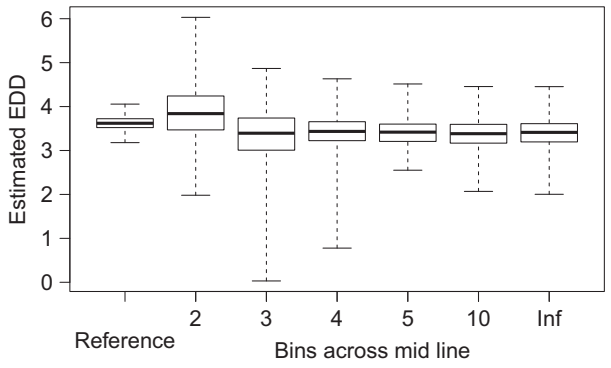

Figure 2. Bootstrapped distributions of estimated effective detection distances using point detection function models applied to different forms of data. Reference indicates unbinned direct distances to first detection position. Mid line models were fitted to distances at which the same records were projected to cross camera's line of sight, with data binned to varying degrees ('Inf' indicates unbinned analysis). Central bars are medians, boxes are interquartile ranges and whiskers are ranges.

Field test

We recorded 13 mammal species, 9 of which had more than 20 distance measurements in one or both habitats (Table 1). The percentage of animals that walked across the midline of the FOV, that is, yielded distance measurements, was higher in the areas with a dense understory (85%) than in areas with a more open understory (74%), and differed slightly between species (Table 1). Using the distance interval measurements, a half-normal detection probability function gave the best fit for most species–habitat combinations except fallow deer and red fox in pine forest and European badger in oak forest, where a hazard-rate function performed marginally better (Table 2). Estimated EDD increased significantly with body mass, as predicted, where a $\log_{10}$ transformation gave the best fit (Fig. 3) both in forests with a dense understory (Least-Squares regression: $F_{1,4} = 23.6$, $P = 0.008$, $R^2_{adj} = 0.82$, $\beta = 2.4$ [95% CI: 1.0–3.8]) and an open understory ($F_{1,4} = 8.2$, $P = 0.045$, $R^2_{adj} = 0.59$, $\beta = 2.4$ [95% CI: 0.1–4.7]).

We then fitted detection probability functions using multiple-covariate distance-sampling models with $\log_{10}$-transformed body mass and habitat as covariates, now using all distance estimates for all species in both habitats. A half-normal model including both covariates had the best fit (AIC = 6439.2; $\beta_{\text{body mass}} = 0.40$; $\beta_{\text{habitat}} = 0.19$), compared to a half-normal model including only body mass as covariate (AIC = 6469.8) or a hazard-rate model including both covariates (AIC = 6530.4). Estimates of EDD from the half-normal covariate model are given in Table 3.

Discussion

Variation in the distance over which passing animals are detected is a major source of error in studies that use camera traps for estimating animal abundance (Rowcliffe et al. 2011). This can be solved by quantifying effective detection distance (EDD). We show that credible estimates of EDD can be obtained from photographs by establishing a line of distance markers in the field of view (FOV) of the camera. This method is a great simplification of previously published methods (Rowcliffe et al. 2011; Caravaggi et al. 2016), and the deployment of markers in front of all cameras did not substantially increase the time spend in the field, or the costs involved in our survey compared to conventional use of camera traps without the estimation of EDD. Our simulations showed that estimates of EDD acquired with this method resemble estimates using the method proposed by

Table 2. Effective Detection Distance (EDD) of terrestrial mammals in two forest types in the Netherlands, estimated with the marker transect method using single-species, single-habitat point detection models.

	Dense understory			Open understory		
	AIC[1]			AIC[1]		
Species	Half-normal	Hazard rate	EDD m (SE)	Half-normal	Hazard rate	EDD m (SE)
Pine marten	44.1	46.1	2.73 (0.30)	74.5	76.6	3.86 (0.35)
Cat				57.5	60.2	4.81 (0.63)
Hare				391.0	400.9	4.77 (0.21)
Fox	94.7	91.8	3.45 (1.13)	245.7	251.5	4.37 (0.25)
Badger				148.1	146.2	7.38 (0.51)
Roe deer	250.6	252.4	5.95 (0.35)	1640.2	1654.7	6.11 (0.15)
Fallow deer	349.3	348.0	7.24 (0.77)			
Wild boar	1616.8	1649.9	5.40 (0.11)			
Red deer	1327.5	1332.7	8.45 (0.27)			

Only species with more than 20 distance measurements per habitat type were included.
[1]EDD estimates are given for the best performing model, highlighted in grey.

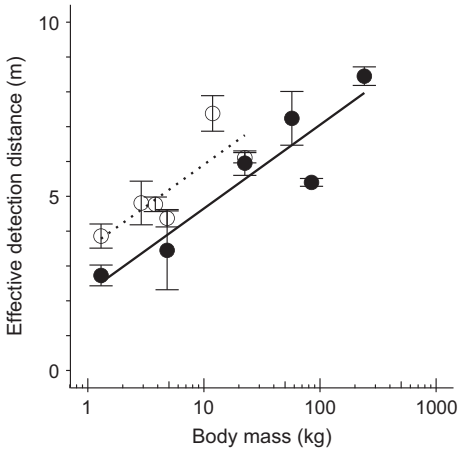

Figure 3. Relationship between the Effective Detection Distance (EDD) estimated with single-species, single-habitat detection functions based on distance intervals obtained from camera trap images using the marker method and body mass of the species. Lines represent linear regression fits for forests with dense understory (filled symbols, solid line) and with open understory (open symbols, dotted line). Whiskers are standard errors.

Table 3. Effective Detection Distance (EDD) of terrestrial mammals in camera trap surveys in two forest types in the Netherlands estimated with the marker transect method using multiple-covariate point models with $\log_{10}$ body mass and habitat as covariates, using all measurements from all species.

Species[1]	Dense understory EDD m (SE)	Open understory EDD m (SE)
Squirrel	2.40 (0.17)	2.90 (0.14)
Hedgehog	2.79 (0.15)	3.37 (0.12)
Polecat	2.90 (0.14)	3.50 (0.12)
Pine marten	3.05 (0.14)	3.68 (0.11)
Stone marten	3.19 (0.13)	3.85 (0.11)
Cat	3.51 (0.12)	4.24 (0.10)
Hare	3.69 (0.11)	4.45 (0.09)
Fox	3.84 (0.11)	4.63 (0.09)
Badger	4.50 (0.09)	5.43 (0.08)
Roe deer	5.03 (0.08)	6.07 (0.07)
Fallow deer	5.92 (0.07)	7.11 (0.06)
Wild boar	6.34 (0.07)	7.58 (0.06)
Red deer	7.55 (0.06)	8.88 (0.05)

[1]Species are ordered by body mass. Species for which a single-species, single-habitat estimate of EDD is available in Table 2 are highlighted in bold.

Rowcliffe et al. (2011) if at least five intervals were used. We obtained credible EDD estimates for 13 different mammal species in two different habitats; estimated EDD increased with species body mass and – to a lesser degree-vegetation openness.

We found that the EDD increased with body mass (Fig. 3), consistent with expectations based on greater emission of heat by larger animals (Mcnab 1980). Similar relationships were found for mammals in Peru (Tobler et al. 2008) and in Panama (Rowcliffe et al. 2011). Scaling of EDD with body mass shows that uncorrected photographic capture rates yield overestimates of relative abundance for large species for which sampling effort is effectively larger. This scaling seems to be corresponding to a $\log_{10}$ transformation of body mass, which is also consistent with previous findings (Tobler et al. 2008; Anile and Devillard 2016). We used estimates of body mass from the global PanTHERIA database (Jones et al. 2009), which might differ from the actual body mass of the local populations, thus introducing error. Therefore, we advise to use body mass estimates obtained from local populations. If age or sex can be distinguished from the

camera trap footage, using age- and sex-specific estimates of body mass can further improve precision.

Many camera-trapping studies do not correct for differences between habitats, implicitly assuming that sampling efficiency of camera traps is constant across habitats (e.g., Rovero and Marshall 2009; Manzo et al. 2012). Our field test demonstrates that differences between habitats can be large – 20% decrease in closed compared to open vegetation in our analysis – and that not accounting for these differences produces biases. For example, apparent differences in habitat use might simply result from vegetation-related differences in detection distance. Avoiding or pruning of vegetation in the FOV may reduce the difference in detectability between sites to some degree, but not entirely. Differences in detection distance in different habitats can be especially problematic when capture rates from camera traps are used to study habitat selection or other variables which are linked to the habitat (Sollmann et al. 2013). Estimating EDD per habitat type and correcting capture rates accordingly can reduce bias in habitat selection studies that use camera trap data.

Our method for estimating EDD relies on the assumption that the distance at which animals cross the midline correlates with the distance at which animals trigger the camera. Our simulation showed that this assumption holds if animals move in a random direction compared to the line of sight of the camera. However, it might no longer hold if animals for some reason tend to always approach from one particular angle. This problem can be overcome by averaging measurements over multiple camera locations. The assumption of random movement of animals compared to the camera position is essential for estimating relative abundance (Sollmann et al. 2013) as well as for estimating density using the random encounter model (REM; Rowcliffe et al. 2008, 2013). Studies using these methods rely on camera placement in random positions, which ensures random movement of animals relative to the camera position. Therefore, our assumptions should hold for camera traps that are deployed for these study purposes, and our method of estimating EDD should give reasonable estimates accordingly.

We found that a minimum of five distance intervals was sufficient for obtaining reliable estimates of EDD (Fig. 2), but this was based on a simulation with a simple detection probability without expansion terms. In reality, detection probability might follow a more complex distribution. For example, detectability at distance zero may be <100% when camera trigger speed is low and animal movement speed is fast, resulting in short-distance detections without photographs of animals and, thus, species-specific distance measurements. In these situations, more precise measurements are needed to model the detection probability. Five distance intervals should thus be considered as a minimum, more is advisable.

Our approach for estimating EDD can be used in the REM for estimating absolute population density (Rowcliffe et al. 2008, 2011). So far, most studies using the REM used a proxy to estimate EDD, for example, by moving in front of the camera themselves (Cusack et al. 2015), or by using a domesticated animal, such as a cat (Manzo et al. 2012). However, our results show that EDD scales with body mass. Thus, the densities found by Manzo et al. (2012) are most probably underestimates, as they used EDD estimated for a domestic cat to estimate pine marten densities, while EDD for pine marten is smaller (Table 2).

While most animals ignored the marking sticks, like the red fox in Figure 1, some sniffed at or chewed on the sticks (especially ungulates and carnivores). Because such responses were uncommon, we consider the image sequences obtained using our method suitable for measuring activity and behaviour. However, the sticks could pose a problem for researchers interested in carnivore or ungulate behaviour. A possible way to overcome behavioural problems could be to take photographs that include markers during the setup or removal of the camera trap, but not leave any markers during the actual deployment (Caravaggi et al. 2016). These photographs can then be used as a reference to overlay all other photographs to measure the distance category at which each animal passes. This might, however, decrease the precision of detection distances as it can be difficult to estimate the right distance interval without physical reference points in front of or behind animals.

Our method allows researchers to correct for differences in capture rate related to variation in EDD, but not for biases caused by differences in the width of the FOV between studies related to the model of camera trap used, openness of the vegetation or size of the species (Rowcliffe et al. 2011). This problem can be overcome by considering only animals that cross the midline of the FOV for calculating capture rates, and discarding all observations of animals that do not cross the line. In essence, the sampling is then reduced to a line. A major advantage of this approach is that the capture rates obtained from this line only need to be corrected for EDD and day range (the distance that animals travel daily) to estimate density (Rowcliffe et al. 2016), just as in line-transect estimation from indirect sign using the Formozov-Malyshev-Pereleshin formula (Stephens et al. 2006). Note that this is equivalent to an REM with a detection angle of zero (Rowcliffe et al. 2008).

In conclusion, our method could facilitate the use of camera traps for estimating relative abundance or density of animal species of which individuals cannot be identified, reducing the bias in relative abundance or density estimates that is due to differences in sampling effort between species and habitats. Our method can be applied by scientists and conservationists all over the world with

limited extra effort. We advise to always deploy camera traps with markers – at least during the setup – as to create the possibility to correct capture rates.

Acknowledgements

We thank the members of the CameraTrapLab at the Resource Ecology Group of Wageningen University for discussion; all landowners for permissions; David L. Miller for support for the *mrds* package; three anonymous reviewers for feedback and the Netherlands Ministry of Health, Welfare and Sport for funding.

Conflict of Interest

The authors declare no conflict of interests.

References

Anile, S., and S. Devillard. 2016. Study design and body mass influence RAIs from camera trap studies: evidence from the Felidae. *Anim. Conserv.* **19**, 35–45.

Buckland, S. T., D. R. Anderson, K. P. Burnham, J. L. Laake, D. L. Borchers, and L. Thomas. 2001. *Introduction to distance sampling*. Oxford University Press, Oxford.

Buckland, S. T., E. A. Rexstad, T. A. Marques, and C. S. Oedekoven. 2015. *Distance sampling: methods and applications*. Springer International Publishing, Cham, Switzerland.

Caravaggi, A., M. Zaccaroni, F. Riga, S. C. Schai-Braun, J. T. A. Dick, W. I. Montgomery, et al. 2016. An invasive-native mammalian species replacement process captured by camera trap survey random encounter models. *Remote Sens. Ecology Conserv.* **2**, 45–58.

Carbone, C., S. Christie, K. Conforti, T. Coulson, N. Franklin, J. R. Ginsberg, et al. 2001. The use of photographic rates to estimate densities of tigers and other cryptic mammals. *Anim. Conserv.*, **4**, 75–79.

Cusack, J. J., A. Swanson, T. Coulson, C. Packer, C. Carbone, A. J. Dickman, et al. 2015. Applying a random encounter model to estimate lion density from camera traps in Serengeti National Park, Tanzania. *J. Wildl. Manag.* **79**, 1014–1021.

Jones, K. E., J. Bielby, M. Cardillo, S. A. Fritz, J. O'dell, C. D. L. Orme, et al. 2009. PanTHERIA: a species-level database of life history, ecology, and geography of extant and recently extinct mammals. *Ecology* **90**, 2648.

Karanth, K. U., and J. D. Nichols. 1998. Estimation of tiger densities in India using photographic captures and recaptures. *Ecology* **79**, 2852–2862.

Kays, R., B. Kranstauber, P. Jansen, C. Carbone, M. Rowcliffe, T. Fountain, et al. 2009. Camera traps as sensor networks for monitoring animal communities. 2009. IEEE 34th Conference on Local Computer Networks, LCN 2009, Zurich. 811–818.

Kelly, M. J., and E. L. Holub. 2008. Camera trapping of carnivores: trap success among camera types and across species, and habitat selection by species, on Salt Pond Mountain, Giles County, Virginia. *Northeast. Nat.* **15**, 249–262.

Laake, J. L., D. L. Borchers, L. Thomas, D. L. Miller, and J. R. B. Bishop. 2015. mrds: Mark-Recapture Distance Sampling. R package version 2.1.14 ed.Avaliable at: http://CRAN.R-project.org/package=mrds (accessed February 10, 2016).

Manzo, E., P. Bartolommei, J. M. Rowcliffe, and R. Cozzolino. 2012. Estimation of population density of European pine marten in central Italy using camera trapping. *Acta Theriologica.* **57**, 165–172.

Marques, F. F. C., and S. T. Buckland. 2003. Incorporating covariates into standard line transect analyses. *Biometrics* **59**, 924–935.

Mcnab, B. K. 1980. On Estimating Thermal Conductance in Endotherms. *Physiol. Zool.* **53**, 145–156.

Meek, P. D., G. Ballard, A. Claridge, R. Kays, K. Moseby, T. O'brien, et al. 2014. Recommended guiding principles for reporting on camera trapping research. *Biodivers. Conserv.* **23**, 2321–2343.

R Core Team. 2015. R: A language and environment for statistical computing. Vienna, Austria: R Foundation for Statistical Computing. Avaliabe at: URL http://www.R-project.org/(accessed February 10, 2016).

Rovero, F., and A. R. Marshall. 2009. Camera trapping photographic rate as an index of density in forest ungulates. *J. Appl. Ecol.* **46**, 1011–1017.

Rovero, F., F. Zimmermann, D. Berzi, and P. Meek. 2013. "Which camera trap type and how many do I need?" A review of camera features and study designs for a range of wildlife research applications. *Hystrix* **24**, 148–156.

Rowcliffe, J. M., and C. Carbone. 2008. Surveys using camera traps: are we looking to a brighter future? *Anim. Conserv.* **11**, 185–186.

Rowcliffe, J. M., J. Field, S. T. Turvey, and C. Carbone. 2008. Estimating animal density using camera traps without the need for individual recognition. *J. Appl. Ecol.* **45**, 1228–1236.

Rowcliffe, J. M., C. Carbone, P. A. Jansen, R. Kays, and B. Kranstauber. 2011. Quantifying the sensitivity of camera traps: an adapted distance sampling approach. *Methods Ecol. Evol.* **2**, 464–476.

Rowcliffe, J. M., Kays, R., C. Carbone, and P. A. Jansen. 2013. Clarifying assumptions behind the estimation of animal density from camera trap rates. *J. Wildl. Manag.* **77**, 876–876.

Rowcliffe, J. M., P. A. Jansen, R. Kays, B. Kranstauber, and C. Carbone. 2016. Wildlife speed cameras: measuring animal travel speed and day range using camera traps. *Remote Sens. Ecology Conserv.* **2**, 84–94.

Sollmann, R., A. Mohamed, H. Samejima, and A. Wilting. 2013. Risky business or simple solution - Relative abundance indices from camera-trapping. *Biol. Conserv.* **159**, 405–412.

Stephens, P. A., O. Y. Zaumyslova, D. G. Miquelle, A. I. Myslenkov, and G. D. Hayward. 2006. Estimating population density from indirect sign: Track counts and the Formozov-Malyshev-Pereleshin formula. *Anim. Conserv.* **9**, 339–348.

Thomas, L., S. T. Buckland, E. A. Rexstad, J. L. Laake, S. Strindberg, S. L. Hedley, et al. 2010. Distance software: design and analysis of distance sampling surveys for estimating population size. *J. Appl. Ecol.* **47**, 5–14.

Tobler, M. W., S. E. Carrillo-Percastegui, R. Leite Pitman, R. Mares, and G. Powell. 2008. An evaluation of camera traps for inventorying large- and medium-sized terrestrial rainforest mammals. *Anim. Conserv.* **11**, 169–178.

Wilson, G. J., and R. J. Delahay. 2001. A review of methods to estimate the abundance of terrestrial carnivores using field signs and observation. *Wildl. Res.* **28**, 151–164.

Supporting Information

Additional supporting information may be found online in the supporting information tab for this article.

Figure S1. Bootstrapped distributions of estimated effective detection distances using line-detection function models applied to different forms of data. Reference indicates unbinned direct distances to first detection position. Midline models were fitted to distances at which the same records were projected to cross camera's line of sight, with data binned to varying degrees ('Inf' indicates unbinned analysis). Central bars are medians, boxes are interquartile ranges and whiskers are ranges.

Table S1. Habitat type, year of measurement, location and number of camera deployments of the eight field sites.

